# Wide-gap Couette flows of dense emulsions: Local concentration measurements, and comparison between macroscopic and local constitutive law measurements through magnetic resonance imaging

G. Ovarlez,[1] S. Rodts,[1] A. Ragouilliaux,[1] P. Coussot,[1] J. Goyon,[2] and A. Colin[2]
[1]*Université Paris Est-Institut Navier, LMSGC (LCPC-ENPC-CNRS) 2, allée Kepler, 77420 Champs-sur-Marne, France*
[2]*LOF, Université Bordeaux 1, UMR CNRS-Rhodia-Bordeaux 1 5258, 33608 Pessac cedex, France*
(Received 20 May 2008; published 10 September 2008)

Flows of dense emulsions show many complex features among which long range nonlocal effects pose a problem for macroscopic characterization. In order to get around this problem, we study the flows of several dense emulsions, with droplet size ranging from 0.3 to 40 $\mu$m, in a wide-gap Couette geometry. We couple macroscopic rheometric experiments and local velocity measurements through magnetic resonance imaging (MRI) techniques. As concentration heterogeneities are expected in the wide-gap Couette flows of multiphase materials, we also designed a method to measure the local droplet concentration in emulsions with a MRI device. In contrast to dense suspensions of rigid particles where very fast migration occurs under shear in wide-gap Couette flows, we show that no migration takes place in dense emulsions even for strains as large as 100 000 in our systems. As a result of the absence of migration and of finite size effect, we are able to determine very precisely the local rheological behavior of several dense emulsions. As the materials are homogeneous, this behavior can also be inferred from purely macroscopic measurements. We thus suggest that properly analyzed purely macroscopic measurements in a wide-gap Couette geometry can be used as a tool to study the local constitutive laws of dense emulsions. All behaviors are basically consistent with Herschel-Bulkley laws of index 0.5. The existence of a constitutive law accounting for all flows contrasts with previous results obtained within a microchannel by Goyon *et al.* [Nature (London) **454**, 84 (2008)]: the use of a wide-gap Couette geometry is likely to prevent here from nonlocal finite size effects; it also contrasts with the observations of Bécu *et al.* [Phys. Rev. Lett. **96**, 138302 (2006)]. We also evidence the existence of discrepancies between a perfect Herschel-Bulkley behavior and the observed local behavior at the approach of the yield stress due to slow shear flows below the apparent yield stress in the case of a strongly adhesive emulsion.

DOI: 10.1103/PhysRevE.78.036307 PACS number(s): 47.57.Bc, 83.80.Iz, 47.55.−t

## I. INTRODUCTION

Emulsions are mixtures of two immiscible fluids consisting of droplets of one phase dispersed into the other, stabilized against coalescence by surfactant. At low droplets volume fraction, the emulsions have basically a Newtonian behavior [1]. When the volume fraction of the dispersed phase is increased, droplets come into contact. If a small stress is applied to a dense emulsion, the interfaces between the droplets can be strained to store surface energy; it results in an elastic response [1]. Above a yield stress, they flow as a result of droplets rearrangements [1]. The flow behavior of dense emulsions can be measured in classical rheological experiments, and seems to be well represented by a Herschel-Bulkley model $\tau(\dot{\gamma})=\tau_c+\eta_{HB}\dot{\gamma}^n$; in monodisperse emulsions, the exponent $n$ has been found to vary between 2/3 and 1/2 for volume fractions varying between 0.58 and 0.65 [2]. At first glance, dense emulsions behavior thus seems to be well understood and modeled.

However, it has been shown recently that the behavior of dense emulsions [3–5], and more generally of pasty materials [6,7], may be much more complex than what can be inferred from simple rheometric experiments, particularly at the approach of the yield stress. The reason is that the flow behavior of materials is usually studied in viscosimetric flows [6], in which one measures macroscopic quantities [a torque $T(\Omega)$ vs a rotational velocity $\Omega$]. A constitutive law relating the shear stress $\tau(\dot{\gamma})$ to the shear rate $\dot{\gamma}$ in any flow can then be derived easily from these macroscopic measurements provided that the flow is homogeneous. However, in complex fluids, this last requirement may not be fulfilled as the flow may be localized, as observed in many pasty materials [3,6,8–12], even in the cone-and-plate geometry [8]. Another problem of importance, that can complicate the analysis of the rheological data, is the existence of slippage of dense emulsions at the walls [4,5,13] even with slightly roughened walls [4].

These problems can be gotten-around by coupling macroscopic torque measurements and local measurements of the shear rate, e.g., through magnetic resonance imaging (MRI) techniques [9], optical methods [5] or sound methods [3], in order to account for these heterogeneities and to get a proper constitutive law. Local measurements in dense emulsions have recently yielded surprising results [3–5]: in some emulsions, it is impossible to find a single constitutive law compatible with all flows. The constitutive law of the material then seems to depend on the velocity at the inner cylinder in a Couette cell [3,5] or the pressure gradient in a Poiseuille cell [4]. Three main reasons have been evoked to explain the apparent absence of a constitutive law: thixotropy, nonlocal effects, and shear-induced migration of the droplets.

Thixotropy may be a cause from the apparent absence of a constitutive law. Long times may indeed be needed to reach a steady state. When the measurements are not performed in this steady state, it may then leave the idea that different laws are required to describe the flow of the sample.

 

Such long times to reach a steady state have been evidenced in some experiments dealing with highly adhesive emulsion [3,11,14]. Importantly, Bécu *et al.* [3], although they claim to have reached a steady state, were unable to account for the flows of their adhesive emulsion with a single constitutive law. Note that we will study again the emulsion of Bécu *et al.* [3] in this paper.

The apparent absence of a single local constitutive law may also be the signature of nonlocal phenomena. Picard *et al.* [15] have actually proposed a nonlocal model to describe the flows of jammed materials (and thus dense emulsions), based upon the cooperativity of the flow. In these systems, flow occurs via a succession of elastic deformation and irreversible plastic events. These localized plastic events induce a relaxation of the stress on the whole system. Their zone of influence is quantified by a length $\xi$. In the presence of high stress gradient or in the vicinity of a surface, this process creates nonlocal effects: indeed, in these situations, the rate of rearrangements of the neighboring fluid differs from what would be the bulk rearrangement rate. As a consequence, these effects affect drastically the rheological behavior when $\xi$ is comparable to the size of the confinement. Such behavior has been recently pointed out by Goyon *et al.* [4]. From experimental data, the authors show that the cooperativity length $\xi$ is zero below the jamming concentration $\phi_m$ and is typically a few oil droplet diameters above $\phi_m$. Using a wide gap should then prevent us from being sensitive to these nonlocal effects. We will check this feature by studying the flows of the Goyon *et al.* [4] emulsion in this paper.

Particle migration may also be a cause for the apparent lack of a local constitutive law [12]. In multiphase materials, wide-gap Couette flows are indeed known to lead to concentration heterogeneities due to shear-induced migration of the dispersed elements toward the low shear zones. The migration of deformable particles, and particularly drops, has been much less studied than the one of rigid particles. Single droplets have been found to migrate away from the rigid walls in any shear flow, due to asymmetric flows around deformed droplets [16]. This leads to an equilibrium position somewhere between the walls, exactly at the center of the gap in the case of a narrow-gap Couette geometry, nearer from the inner cylinder in the case of a wide-gap Couette geometry [17]. When dealing with a dilute emulsion, it has been observed, in contrast with dilute suspensions of rigid particles, that the equilibrium distribution of droplets is parabolic around a position that is near the equilibrium position of single droplets [17–19]. The theoretical explanation is that all particles would tend to accumulate at the same equilibrium position between the walls, but their distribution is broadened by their binary collisions (this second process may be modeled as it is for rigid particles). Only rather dilute emulsions (up to 10% of droplets) have been studied so far, and nothing is known about what happens for higher droplet concentrations. In this case, one would expect the wall effect on the droplet migration to be negligible compared to the effect of the interactions between droplets; then, one would expect migration to produce the same effects as in suspensions, with the same kinetics as it has basically the same physical origin. We can thus expect that relevant information for migration in dense emulsions can be found in the literature dealing with suspensions of rigid particles. In suspensions of noncolloidal rigid particles, migration has been observed in many situations: wide-gap Couette flows [12,20–23], parallel-plate flows [24], pipe flows [25,26]. In wide-gap Couette flows, the consequence of migration is an excess of particles near the outer cylinder. Migration is related to the shear-induced diffusion of particles [22,23]: the gradients in shear rate that exist in all but the cone and plate geometry generate a particle flux toward the low shear zones (the outer cylinder in the case of the Couette geometry), which is counterbalanced by a particle flux due to viscosity gradients. In an alternative model [27,28], particle fluxes counterbalance the gradients in normal stresses. Most experiments [20,21,23] observe that migration in suspensions of volume fraction up to 55% is rather slow, in accordance with its diffusive origin. However, it was recently found in a Couette geometry that in the case of very dense suspensions (up to 60%), which exhibit an apparent yield stress, migration is almost instantaneous [12] (it lasts for a few revolutions) so that it may be unavoidable. A reason for this very fast kinetics may be that particles are closely packed together: any shear may then push the particles toward the outer cylinder with an instantaneous long range effect on the particle concentration. Migration may then be expected to be very fast for dense emulsions exhibiting a yield stress, i.e., in which droplets are in contact as the particles in the very dense suspensions of [12].

In this paper, we address the questions of the existence and the determination of a local constitutive law for the flows of dense emulsions. In this aim, we use a wide-gap Couette cell to avoid nonlocal effects, and we study in detail the question of shear-induced droplet migration in these systems. We also take care of performing our experiments in a steady state. We propose to couple macroscopic measurements and local measurements of concentration and velocity through MRI techniques during the wide-gap Couette flows of dense emulsions. A method designed to measure the local droplet concentration in emulsions is developed, and we seek the occurrence of migration on many formulations. Local measurements of the constitutive law are then compared to purely macroscopic measurements.

In Sec. II, we present the materials and the experimental setup. We present the concentration profiles obtained on all materials after long-time experiments in Sec. III A. The velocity profiles are shown in Sec. III B. The macroscopic rheometrical measurements are displayed in Sec. III C, and a purely macroscopic determination of the constitutive law is presented. The results are analyzed in Sec. III D: we determine locally the constitutive law of the material from the velocity profiles, and we compare macroscopic and local measurements of the constitutive law.

## II. MATERIALS AND METHODS

### A. Emulsions

As the time scale for the occurrence of migration is *a priori* very sensitive to the droplet size $R$ (if a diffusive process is involved, it should scale as $1/R^2$), we study dense emulsions of four different sizes: 0.3, 1, 6.5, and 40 $\mu$m.

Moreover, as problems in defining a local constitutive law seem to be linked to the adhesion properties of the droplets [3], we took care of formulating adhesive and nonadhesive emulsions. Note in particular that we study the emulsions of Bécu *et al.* [3] and Goyon *et al.* [4], which posed problems in defining a single local constitutive law accounting for all their flows.

The 0.3 $\mu$m emulsion is the adhesive emulsion of Bécu *et al.* [3]; nearly monodisperse oil in water emulsions are prepared by shearing a crude polydisperse emulsion, composed of castor oil droplets in water stabilized by sodium dodecyl sulfate (SDS), within a narrow gap of 100 $\mu$m [29]. The surfactant concentration within the aqueous phase is set to 8 wt %, which leads to an adhesive emulsion [3]. The oil volume fraction is 73%, and the droplet mean diameter is 0.3 $\mu$m with a polydispersity of about 20%, which is enough to prevent crystallization.

The 1-$\mu$m emulsion is a nonadhesive emulsion. The preparation of the sample is the same as the one used to get the adhesive 0.3-$\mu$m emulsion. It is composed of silicone oil in water stabilized by sodium dodecyl sulfate (SDS). The surfactant concentration within the aqueous phase is set to 8.5%. The viscosity of the oil is 1 Pa s and the oil volume fraction is 75%.

We prepared adhesive and nonadhesive oil in water emulsions, of 6.5-$\mu$m mean diameter with a polydispersity of about 20%. These emulsions are composed of silicone droplets in a mixture of glycerine and water (50 wt % glycerine, 50 wt % water) stabilized by Brij and trimethyl tetradecyl ammonium bromide, sheared in a narrow-gap Couette cell. The trimethyl tetradecyl concentration within the aqueous phase is set to 1 or 6.5 wt %, which leads to respectively adhesive and non-adhesive emulsions. The oil viscosity is 1 Pa s. The oil volume fraction is 75% in all cases. Note that the nonadhesive 6.5-$\mu$m emulsion is the same as in Goyon *et al.* [4]. Note that the use of glycerol in the continuous phase prevents us from obtaining accurate concentration measurements with the method developed below. Only qualitative results can be inferred from the measurements: in particular, if the intensity profiles are unchanged after a flow, it means that there is no migration.

We finally studied a large droplet brine in oil nonadhesive emulsion, of 40-$\mu$m mean diameter with a polydispersity of about 50%, at an 88% concentration. The emulsion is prepared by progressively adding the brine (solution of $CaCl_2$ at 300 g/l in water) in an oil-surfactant solution [HDF 2000 (total solvent)+sorbitan monooleate at 2%] under a controlled high shear with a Silverson L4RT mixer.

### B. Rheological measurements

#### 1. Display

We carried out experiments with a velocity controlled "magnetic resonance imaging (MRI) rheometer." Experiments are performed within a wide-gap Couette geometry (inner cylinder radius $R_i$=4.1 cm, outer cylinder radius $R_o$ =6 cm, height $H$=11 cm). In order to avoid slip at the walls, sandpaper is glued on the walls. Rheometric measurements are performed with a commercial rheometer (Bohlin C-VOR 200) that imposes either the torque or the rotational velocity (with a torque feedback). The whole geometry is inserted in a 0.5-T vertical MRI spectrometer (24/80 DBX by Bruker). The MRI measurements allow us to get the local orthoradial velocity and the local droplet concentration of the material anywhere in the gap, with a radial resolution of 0.5 mm. For details on the MRI sequence devoted to measure the local velocity and its application to rheology, see [12,30]. A method devoted to obtain the local droplet concentration was developed specifically for this study and is presented hereafter.

#### 2. Concentration measurements

Proton NMR relies on the properties of hydrogen nuclei, which bear a magnetic dipole. In a NMR experiment, the sample is put inside a strong, static, and (as far as possible) homogeneous field $\vec{B}_0$. The magnetization of hydrogen nuclei then tends to align along the static field. The sample develops a nonzero magnetization density $m_0(\vec{r})$ which follows the Curie law:

$$m_0(\vec{r}) = \rho_H(\vec{r}) B_0 \frac{\gamma^2 \hbar^2}{4 k_B T}, \tag{1}$$

where $\rho_H$ is the hydrogen density at position $\vec{r}$, $\gamma$ is the gyromagnetic ratio of hydrogen nuclei, $\hbar$ is the Planck constant, $k_B$ is the Boltzmann constant, and $T$ is the sample temperature. $\rho_H$ can be easily computed for any sample from its chemical formula and its density.

When put out of equilibrium, magnetization of liquids often develops a threefold dynamic behavior combining a precession motion around the permanent field of the magnet, and two relaxation processes: a monoexponential decay of transverse components of $\vec{m}_0(\vec{r})$ with a characteristic time $T_2$, and a monoexponential relaxation of the longitudinal component of $\vec{m}_0(\vec{r})$ towards its equilibrium value, with a characteristic time $T_1$. Nuclear magnetic resonance technique consists of a series of magnetization manipulation and measurements by means of an externally applied additional magnetic field, aiming at getting information about physicochemical properties of the sample. The magnetic resonance imaging extension of NMR permits us to get, as far a possible, a space resolved view of the local magnetization density, and can make such analysis local and nonperturbative.

Because of signal-to-noise ratio limitations, the space resolution of MRI facilities for imaging purposes can never be much better than about one-hundredth of the size of the experimental setup, that is 1 mm in our working conditions, which is much too big to resolve independent droplets. Measuring the water to oil ratio in a sample then requires us to have a way to distinguish oil and water magnetization inside a single pixel of a MRI image.

Up to now, three main discrimination routes were already reported in emulsion literature. The first one relies on the so-called chemical shift difference between water and oil. Actually, the exact precession frequency around the permanent field is closely related to the direct chemical neighborhood of hydrogen atoms. Because all hydrogen nuclei of water are linked to oxygen atoms, and most of the hydrogens

in oily material are linked either to carbon or silicium atoms, water and oil magnetization always exhibits two different precession frequency. This chemical shift is quite small (about 4–4.5 ppm relative difference, whenever carbon or silicon oils are used). Nevertheless, this shift can be accurately observed provided that $\vec{B}_o$ inhomogeneities across the sample have a much smaller amplitude than 4.5 ppm of the mean $B_o$ value (e.g., see the spectrum by Götz and Zick [31]). Indeed, the precession frequency is also proportional to local $\vec{B}_o$ intensity, and one should avoid confusion between the original chemical shift and any spurious one originating from field heterogeneities. Homogeneity constraints can be met when the fluid is embedded in a container with a simple shape. Reported studies making use of the chemical shift contrast then often deal with emulsions that are contained in a simple beaker, or even a cylindrical pipe displayed parallel to $\vec{B}_o$. Quite early results deal with the use of chemical shift imaging (CSI) for a quantitative assessment of oil and fat content in food emulsions [32], or the separation of oil and water components of an emulsion during a filtration process [33]. More recently, Götz and Zick [31] and Hollingsworth and Johns [17] managed to carry out quite well resolved local measurements of water and oil concentrations and/or velocities in model suspensions flowing through a pipe in a laminar regime. Unfortunately, the chemical shift contrast can hardly be transposed in the case of a Couette cell. The geometry is indeed more complex and involves edges between materials with different magnetic susceptibilities, prone to generate strong local field distortions. CSI applications to Couette flow are thus more difficult and actually quite rare. For instance, D'Avila *et al.* [34], who studied the mixing process of oil and water in a horizontal Couette-like device, reported quite long measuring times and only poorly resolved pictures.

A second way to discriminate between water and oil in an emulsion relies on $T_1$ relaxation time. $T_1$ (as well as $T_2$) indeed strongly depends on a wide set of parameters, such as fluid composition, diffusion coefficient, temperature, or the presence of dissolved species. In water and oil, they usually turn out to be quite different. For instance, in our working conditions (0.5-T magnetic field) $T_1$ and $T_2$ usually range between 2 and 3 s in bulk water (depending on water origin and dissolved minerals), while many carbonated and silicon oils exhibit $T_1$ about few 100 ms, and $T_2$ even smaller. Although the use of $T_2$ contrast was already reported as a promising NMR tool of characterizing droplet size in an emulsion [35], previous works involving imaging possibilities of NMR prefer $T_1$ contrast. As compared with chemical shift or $T_2$, $T_1$ physical value and $T_1$ measurement techniques are indeed fairly insensitive to field inhomogeneities. Kauten *et al.* [36] demonstrated this contrast to give quantitative information on the creaming process of an oil-water emulsion. More recently, few works showed its ability to work in more severe conditions. Maricani *et al.* [37] used $T_1$ to measure the fat fraction in an emulsion contained inside the stomach of a human volunteer. Hollingsworth and Johns [17] also reported the use of a $T_1$ based method to follow the droplet migration in a low concentrated emulsion under shearing in a Couette cell.

A third way also used to study the creaming of an emulsion [38] consists of preparing a water-oil emulsion based on deuterium oxide instead of normal water. Because proton NMR is only sensitive to 1H nuclei, NMR or MRI measurements then bring exclusive information on the oil phase.

In our work, we wanted to get independent information on oil and water phase. Field inhomogeneities inside our Couette cell were also in many places of the same order of magnitude as the chemical shift. This was mainly due to the covering of the surfaces of the cell with sandpaper, that was used so as to avoid slip problems. $T_1$ contrast was then regarded as the best contrast source. Although details of our measurement method were quite different than that of Hollingsworth and Johns [17] it was also based on the so-called inversion-recovery technique. Starting from a magnetization in equilibrium state, it consists of putting magnetization upside down by means of an appropriate external field, and then to let it relax towards its equilibrium value. In a homogeneous sample with relaxation time $T_1$ and equilibrium magnetization density $m_o$, the magnetization about the main magnetic field should then read

$$m(t) = m_o(1 - 2e^{-t/T_1}), \tag{2}$$

where $t=0$ at the time of inversion. To perform an accurate analysis, we found it necessary to consider additionally that the initial inversion can never be perfect: the magnetization about the main magnetic field then actually reads

$$m(t) = m_o(1 - Ie^{-t/T_1}), \tag{3}$$

where $I$ reflects the actual inversion conditions: $I$ would be equal to 2 in perfect experimental conditions, but was actually always found to be slightly less than 2. Its exact value and space homogeneity depends on both the hardware and the sample.

In a water-oil emulsion, it is admitted that water and oil behave as two independent phases: the resultant magnetization is then the sum of the individual oil and water magnetization that relax independently. The mean magnetization inside a water-oil emulsion then reads

$$m(t) = \phi^w m_o^w(1 - Ie^{-t/T_1^w}) + \phi^o m_o^o(1 - Ie^{-t/T_1^o}), \tag{4}$$

where $m_o^w$ and $m_o^o$ are the equilibrium magnetization density of bulk water and oil, respectively, $\phi^w$ and $\phi^o$ are the water and oil volume fractions ($\phi^w + \phi^o = 1$), and $T_1^w$ and $T_1^o$ are the longitudinal relaxation time of water and oil, respectively. $I$ is supposed to be the same in oil and water.

From Eq. (4), in order to observe only water droplets in a water in oil emulsion, Hollingsworth and Johns [17] used the fact that there is always a time during this relaxation process when the oil magnetization is zero. They made a MRI picture of $m(t)$ at this time, based on the assumption that $I=2$ everywhere in the sample. However, we think that the accuracy of such a technique may be limited, because a wrong estimation of the actual $I$ factor, if not exactly 2, or a wrong estimation of relaxation times will always lead to a wrong estimation of the time for which the oil magnetization is zero, and then, to an incomplete oil canceling.

Using *in situ* measurements of water and oil relaxation

times, we developed another approach which consists of performing three MRI measurements of the magnetization relaxation, for three carefully chosen waiting times, and then solving an equation system, with $I$ as a free parameter. We then obtain space resolved measurements of $I(\vec{r})$, $\phi^w(\vec{r})m_o^w$, and $\phi^o(\vec{r})m_o^o$ as averaged at the pixel scale. The three waiting times are optimized for each sample in order to minimize the uncertainty on the magnetization values. As compared with the "phase canceling" technique, we calculated that this method is much more accurate, and especially less sensitive to $T_1$ uncertainties when $T_1$ values in water and oil are clearly separated.

In order to get the material volume fraction from Eq. (4), *in situ* measurement of relaxation times were found to be a necessary step of the experimental procedure. Indeed, as far as relaxation phenomena are considered, although water and oil mainly behave as if they would be independent phases, they interact anyway together with the surfactant at the surface of each droplet. Relaxation times in water may then be influenced by the presence of the oil phase. Relaxation times in oil may also differ from that of pure oil because aliphatic chains of surfactant molecules mix with oil in the vicinity of the droplet surface. The sensitivity to the droplet size was reported to be quite dramatic for $T_2$ value in a water-oil emulsion containing a large amount of additional impurities [35]. We believe in such a system that $T_1$ and $T_2$ should qualitatively behave the same. In our samples, which are made of quite pure water and oil phases, the $T_1$ difference between the pure phases and the droplets was found to be of order 10%. This difference is probably too small to provide a quantitative sensitivity of our measurements to droplet size changes in our systems. Anyway, $T_1$ changes, as small as they may be, have to be taken into account for the accuracy of local fraction measurements. Eventually, $T_1$ may also evolve with any small change in the temperature of the sample. That is why before each concentration measurement, the actual relaxation times were measured.

As $T_1$ is sensitive to the details of the local structure of the material, $T_1$ measurements should ideally be space resolved. However, we worked here another way: we used an average $T_1$ measurement in the whole gap of the cell, discriminating water and oil on the basis of their chemical shift (field inhomogeneities were too strong for a CSI-based imaging, but were still OK for $T_1$ measurements). The average $T_1$ values for oil and water were then directly used to process the MRI data. Granted that processed oil and water volume fractions were then always found to be homogeneous within the gap of the cell, we had then an *a posteriori* confirmation that our global $T_1$ measurements were meaningful. One should be aware anyway that if any heterogeneity would have been detected in measured volume fractions, then it would have been necessary to shift to local $T_1$ measurements to ensure very accurate quantitative results; measurements based on the global $T_1$ measurement would, nevertheless, provide a relevant estimation of the volume fractions.

Finally, in order to obtain the local volume fraction $\phi^o(\vec{r})$ and $\phi^w(\vec{r})$ of each phase, it is sufficient to remember that from Eq. (1), $m_o^w = \rho_H^w(B_o\gamma^2\hbar^2/4k_BT)$ and $m_o^o = \rho_H^o(B_o\gamma^2\hbar^2/4k_BT)$. The absolute uncertainty on the concentration measurement performed with this method was found to be of 0.3% from measurements performed on a homogeneous emulsion. Note that when the proton density of the oil phase is not known, the comparison of the $\phi^w(\vec{r})m_o^w$ and $\phi^o(\vec{r})m_o^o$ measurements performed on the homogeneous emulsion (of known volume fraction) allows us to recover its value. Note also that a simple way to check for changes in the local concentration, and to evaluate the amplitude of these changes, consists in comparing the water and oil intensity profiles within the gap after shear to the profiles measured on the emulsion just after loading. These last profiles are performed on a homogeneous emulsion, any change in these profiles induced by shear would then mean that there is migration.

#### *3. Procedures*

In the experiments presented hereafter, we control the rotational velocity of the inner cylinder. For all materials, we first apply a constant rotational velocity of 20–100 rpm until 10 000–90 000 revolutions have been completed. We record the evolution of the velocity profiles and the concentration profiles in time in order to check for the occurrence of migration (see Sec. III A). Afterwards, we measure the stationary velocity profiles and the stationary torque exerted by the material on the inner cylinder for various velocities ranging from 0.1 to 100 rpm (see Secs. III B and III C).

## III. RESULTS

### A. Concentration profiles

In order to search for the occurrence of shear-induced migration in dense emulsions, we sheared all materials for long times. We chose to apply velocities ranging between 20 and 100 rpm; this ensures that in all cases the whole gap is sheared (see Sec. III B). We also checked on the 6.5-$\mu$m emulsions that the same results are obtained when the flow is localized during the experiment (i.e., when the material is sheared at 1 rpm). The 0.3-$\mu$m emulsion was sheared for 10 000 revolutions, the 1-$\mu$m emulsion was sheared for 90 000 revolutions, both 6.5-$\mu$m emulsions were sheared for 35 000 revolutions, and the 40-$\mu$m emulsion was sheared for 20 000 revolutions. The corresponding local strains, extracted from the velocity profiles (see Sec. III B), range between five times the number of revolutions near the inner cylinder, and 0.25 times near the outer cylinder.

In all the experiments, within the experimental uncertainty, we observe that the materials remain homogeneous after shear: there is no observable shear-induced migration. Results for the 0.3-$\mu$m and the 40-$\mu$m emulsion are depicted in Fig. 1. Note also that the relaxation times $T_1$ of the oil and water phases were not observed to change during all the experiments: as pointed out in Sec. II, this is consistent with the fact that the droplet size is unchanged by shear and that all the measurements deal with the same homogeneous suspension. Consistently, optical observations of the droplets after shear did not reveal size changes.

As noted in Sec. I, up to now only rather dilute emulsions have been studied: we cannot compare our results with any result from the literature dealing with emulsions. However,

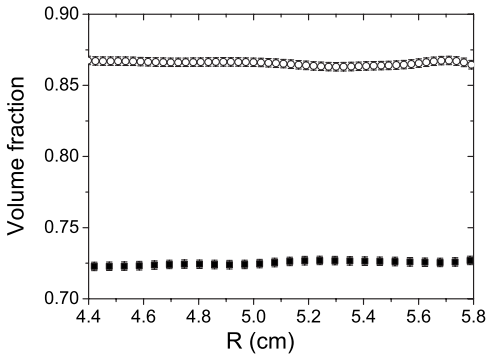


FIG. 1. Concentration profiles observed within the gap of a Couette geometry after shearing a 0.3-$\mu$m adhesive emulsion for 10 000 revolutions (squares), and a 40-$\mu$m nonadhesive emulsion for 20 000 revolutions (open circles).

the relevant mechanism involved in migration of droplets in dense emulsions should be basically the same as in suspensions of rigid particles, namely a shear-induced diffusion of particles. From this model and results from the literature of migration in dense suspension, we can thus infer whether or not migration would have been expected in our systems. In the diffusive model of migration [22,23], the particles undergo a shear-induced diffusion characterized by a self-diffusion coefficient $D=\bar{D}(\phi)\dot{\gamma}a^2$ [39,40], where $\phi$ is the particle volume fraction, $\dot{\gamma}$ is the shear rate, $a$ is the particle size, and $\bar{D}$ is a dimensionless coefficient whose dependence on $\phi$ may theoretically be $\bar{D}(\phi)\propto\phi^2$ for small $\phi$. The gradients in shear rate that exist in a Couette geometry then generate a particle flux towards the outer cylinder, which is counterbalanced by a particle flux due to viscosity gradients. As qualitatively confirmed experimentally [20,41], one would then expect the migration phenomenon to last for a number of revolutions $N_{migr}\propto(R_o-R_i)^3/(\bar{R}a^2\phi^2)$ until a stationary heterogeneous profile is established, where $R_o$ and $R_i$ are, respectively, the outer and inner radius, and $\bar{R}=(R_o+R_i)/2$. Within the frame of this model, we can now evaluate the expected $N_{migr}$ for complete migration in our experiment from experimental results from the literature. Actually, as shown by Ovarlez *et al.* [12] two inconsistent sets of data exist, depending on the concentration: migration has been shown to occur much more rapidly for concentrations above 55%. E.g, for moderately dense suspensions, Corbett *et al.* [20] find $N_{migr}=2000$ revolutions for 140-$\mu$m particles, at $\bar{\phi}=0.4$, with $R_o=1.9$ cm and $R_i=0.95$ cm. In the case of our materials, this would imply a value of $N_{migr}\approx 2.8\times10^8$ revolutions for the 0.3-$\mu$m emulsion, $N_{migr}\approx 2.5\times10^7$ revolutions for the 1-$\mu$m emulsion, $N_{migr}\approx 6\times10^5$ revolutions for the 6.5-$\mu$m emulsions, and $N_{migr}\approx 10\,000$ revolutions for the 40-$\mu$m emulsion. On the other hand, for very dense suspensions, Ovarlez *et al.* [12] found that migration occurs during the first 50 revolutions within the same Couette geometry as ours. This would imply an expected value of $N_{migr}\approx 2.8\times10^7$ revolutions for the 0.3-$\mu$m emulsion, $N_{migr}\approx 2.5\times10^6$ revolutions for the 1-$\mu$m emulsion, $N_{migr}\approx 60\,000$ revolutions for the 6.5-$\mu$m emulsions, and $N_{migr}\approx 1000$ revolutions for the 40 $\mu$m emulsion in our experiments. Let us recall that $N_{migr}$ is the number of revolutions expected for *complete* migration, and that heterogeneities should be observable for a value of $N_{migr}/10$ revolutions (see Abbott *et al.* [41] and Tetlow *et al.* [42] for measurements of transient concentration profiles in suspensions).

If a shear-induced migration mechanism similar to the one observed in suspensions of rigid particles was acting in dense emulsions, we should therefore have observed migration in the 40-$\mu$m emulsion and in the 6.5-$\mu$m emulsions. On the other hand, our experiments cannot be used to conclude directly for the failure of a diffusive model of migration in the case of the smaller droplets (0.3 and 1 $\mu$m), but we can expect to predict what happens in this case from the $a^2$ scaling of the diffusion process if this process is relevant. Even if it is impossible to conclude definitely for the absence of migration for any strain, we can conclude that if a diffusive process acts in dense emulsions, it is much slower than the process involved in dense suspensions of rigid particles. Importantly, our results provide reliable lower bounds for the occurrence of migration in dense emulsions. For practical purposes, in most flows and particularly in most rheometrical studies of dense emulsions, it can therefore be claimed that the emulsions remain homogeneous.

Surprisingly, our results contrast with what was observed by Ovarlez *et al.* [12] in dense suspensions of hard spheres where very fast migration was found to occur. A first reason could be that jamming prevents from migration in dense emulsions. However, it was found that migration in dense suspensions can lead to regions having a concentration higher than the maximum packing fraction $\phi_m$ above which there is no more flow [12]: this shows that jamming does not necessarily prevent migration. Another reason could be that deformability of the particles play a central role. The shear stresses involved in the flow are on the order of 100–200 Pa in all materials, whereas the typical stress due to surface tension ranges between 1000 Pa for the 40-$\mu$m droplets and 120 000 Pa for the 0.3-$\mu$m particles. The droplets may then be poorly deformable (except for the 40-$\mu$m emulsion) under shear, but they must be deformed due to confinement and to their high concentration. In particular they should have flat contacts which may allow the droplets to slip easily past each other; this is a major difference with the suspensions of hard spheres in which any shear may push the particles towards the outer cylinder with an instantaneous long range effect on the particle concentration thanks to the force chains originating from direct frictional contact forces.

Note that consistency of our observations with the modeling of shear-induced migration based on normal stresses is difficult to check as normal stresses in dense emulsions are poorly known. It should be noted, however, that the normal stresses due to surface tension should be of the order of the yield stress [1] in dense emulsions, while normal stresses tend to diverge at the approach of the maximum packing fraction in dense suspensions of rigid particles (this difference is linked to the deformability of the droplets leading to flat contacts as pointed out above). It is thus not unexpected from this point of view that the kinetics of shear induced migration in a Couette flow, which depends on the spatial variation of the first normal stress difference and of the radial normal stress [43], is very fast near the maximum packing

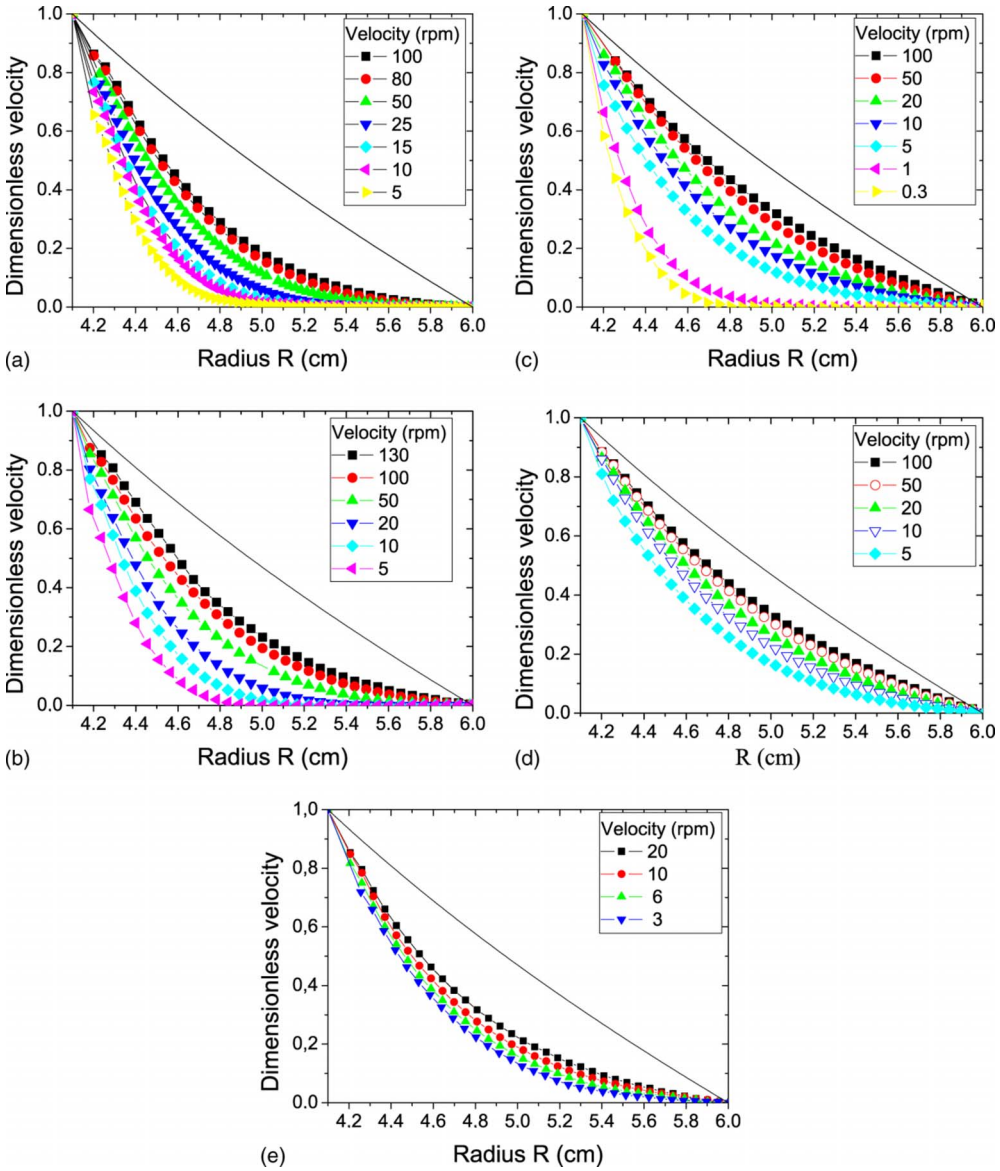


FIG. 2. (Color online) (a) Dimensionless velocity profiles for the steady flows of a 0.3-$\mu$m adhesive emulsion, at various rotational velocities ranging from 5 to 100 rpm; the line is the theoretical dimensionless velocity profile for a Newtonian fluid. (b) The same plot for a 1-$\mu$m nonadhesive emulsion. (c) The same plot for a 6.5-$\mu$m adhesive emulsion. (d) The same plot for a 6.5-$\mu$m nonadhesive emulsion. (e) The same plot for a 40-$\mu$m nonadhesive emulsion.

fraction in suspensions of hard spheres while it would have to remain slow in dense emulsions. Anyway, it is not possible to be more quantitative at this stage and to state if migration would have been expected to occur within this picture in our experimental conditions.

### B. Velocity profiles

In these experiments, after a 5-min preshear at 100 rpm, we measured the velocity profiles at various rotational velocities. In all systems, the stationary velocity profiles were found to develop within a few seconds and to remain stable for hours. This means that these systems are not thixotropic [6]. In the case of the 0.3-$\mu$m adhesive emulsion, this contrasts with the long time evolution of the velocity profiles observed by Bécu *et al.* [3]; we will comment on this point below. The stability of the velocity profiles is also consistent with the absence of shear-induced droplet migration in all systems: as the behavior of dense emulsions depends on their concentration, changes in the concentration profiles in time would have led to changes in the velocity profiles in time. This feature is important: in the absence of a method to measure the concentration profiles, the stability of the velocity profiles can be used as a proof of the absence of migration as long as the migration process is not nearly instantaneous.

In Fig. 2, we plot the dimensionless velocity profiles for the steady flows of all the emulsions for various rotational velocities ranging from 0.3 to 100 rpm.

The 1-$\mu$m nonadhesive emulsion, the 6.5-$\mu$m adhesive and nonadhesive emulsions, and the 40-$\mu$m nonadhesive emulsion share a common behavior. MRI measurements

show that the velocity profiles are curved, and that they occupy only a small fraction of the gap at low rotational velocities (Fig. 2): in this case, the velocity tends to zero within the measurement uncertainty at some radius before the outer cylinder. The fraction of the material that is sheared increases with the rotational velocity. Beyond a critical velocity $\Omega_c$, that depends on the emulsion and is of order 3 rpm in the case of the 6.5-$\mu$m adhesive emulsion [Fig. 2(c)], or of the order 50 rpm in the case of the 1-$\mu$m nonadhesive emulsion [Fig. 2(b)], the whole sample is sheared. This shear localization is a classical feature of yield stress fluid flows in Couette geometry where the shear stress is a decreasing function of the radius: the flow must stop at a radius $R$ such that the shear stress equals the material yield stress at this place. Note that this behavior is not evidenced for the nonadhesive 6.5-$\mu$m emulsion and for the nonadhesive 40-$\mu$m emulsion: this is simply due to the fact that the applied rotational velocities are too high to probe this behavior.

When all the gap is sheared, the velocity profiles are clearly different from those of a Newtonian fluid (Fig. 2). The curvature we observe is due to the use of a wide-gap Couette geometry and is actually typical of shear-thinning fluid: the shear rate decreases more rapidly within the gap (i.e., when the shear stress decreases) than for a Newtonian fluid. The shear rate may vary here by a factor 20 within the gap while it would vary by a factor 2.1 for a Newtonian fluid in this geometry [this factor 2.1 is simply the ratio between the shear stress at the inner cylinder and the shear stress at the outer cylinder; see Eq. (5) in Sec. III C]. This implies that in the analysis of macroscopic experiments, one cannot simply compute a mean shear rate within the gap to characterize the flow.

Finally, note that no data can be recorded close to the inner cylinder. As a consequence, the expected absence of wall slip (due to the use of rough surfaces of roughness larger than the droplet size) cannot be proved at this stage. It can only be observed that the extrapolation of the dimensionless velocity profiles to a value of 1 at the inner cylinder is reasonable, and that wall slip—if any—should be of a limited amount of order 5% or less. We will show in Sec. III D that it is possible to infer the emulsion velocity at the walls from its local constitutive law, and that wall slip—if any—is actually less than 1% of the inner cylinder velocity.

At first sight, the 0.3-$\mu$m adhesive emulsion presents the same behavior as the other samples. The velocity profiles are curved, and they occupy only a small fraction of the gap at low rotational velocities. However, focusing on the low velocities part and thus very low shear rates part of the profiles, a striking behavior is evidenced in the semilogarithmic scale figure [Fig. 3(a)]. A slope break in the profile is evidenced at a given radius inside the gap. The velocity then starts to decrease very slowly with the radius. There is then a large zone of the material in which there remains a very slow flow. This behavior is reminiscent of the one observed previously by Bécu *et al.* [3] and by Ragouilliaux *et al.* [11,14] in adhesive emulsions (this behavior will be shortly commented on Sec. III D). These slowly varying slow flows occur here for velocities lower than a few 100 $\mu$m s$^{-1}$. This behavior seems to be a specific feature of the strongly adhesive 0.3-$\mu$m emulsion. We measured velocity as low as 10 $\mu$m s$^{-1}$ at the approach of flow stoppage in the 1-$\mu$m nonadhesive and 6.5-$\mu$m adhesive emulsion [Figs. 3(b) and 3(c)] but did not observe any slope break in these cases: there is no evidence of any slow flow in the apparently jammed zones in these emulsions.

In the following, we build the constitutive laws of the emulsions accounting for their flow properties. To get this information, we use two different methods. First, focusing on the macroscopic measurements, we present an experimental procedure allowing us to get a relationship between local values of the shear stress and the shear rate by measuring only macroscopic quantities (Sec. III C). Second, we analyze in detail the velocity profiles and extract a local constitutive law by differentiating the velocity field to get the local shear rate (Sec. III D).

### C. Macroscopic characterization

In this section, we present the macroscopic rheometric measurements (torque vs rotational velocity). We then show that it is possible to extract the constitutive law of the material from a proper analysis of this set of purely macroscopic data only provided that the material is homogeneous (absence of migration) and that there is no wall slip, which is what we have ensured.

For each rotational velocity $\Omega$, we have measured the torque exerted on the inner cylinder vs time until a stationary state is reached [see inset of Fig. 4(a) for the 0.3-$\mu$m adhesive emulsion]. We observe that for each rotational velocity, a stationary state is reached for a strain of a few unities, consistently with the absence of evolution of the velocity profiles in time. In Fig. 4(a) we plot the stationary torque vs the rotational velocity for the steady flows of the 0.3-$\mu$m adhesive emulsion.

We observe that the apparent flow curve of the material is that of a yield stress shear-thinning fluid. As we have shown in Sec. III A that the material is homogeneous, we are allowed to use these macroscopic data to infer the constitutive law of the material. Because of the strong stress and shear rate heterogeneities, in particular shear localization, standard formula relating simply the torque and rotational velocity values to a mean shear stress and a mean shear rate cannot be used. However, it is possible to analyze the macroscopic data to account for these heterogeneities and to obtain the unique constitutive law consistent with this set of purely macroscopic data. The method used to analyze the wide-gap Couette rheometric data in order to obtain the constitutive law of the material is detailed, e.g., in [6], we give here the main steps. First, it has to be noted that the shear stress distribution $\tau(R)$ within the gap at a radius $R$ is known whatever the constitutive law of the material; it reads

$$\tau(R) = T/(2\pi HR^2), \tag{5}$$

where $T$ is the torque and $H$ is the height of the Couette geometry. Then, the local shear rate $\dot{\gamma}(R)$ is related to the rotational velocity $\Omega$ through

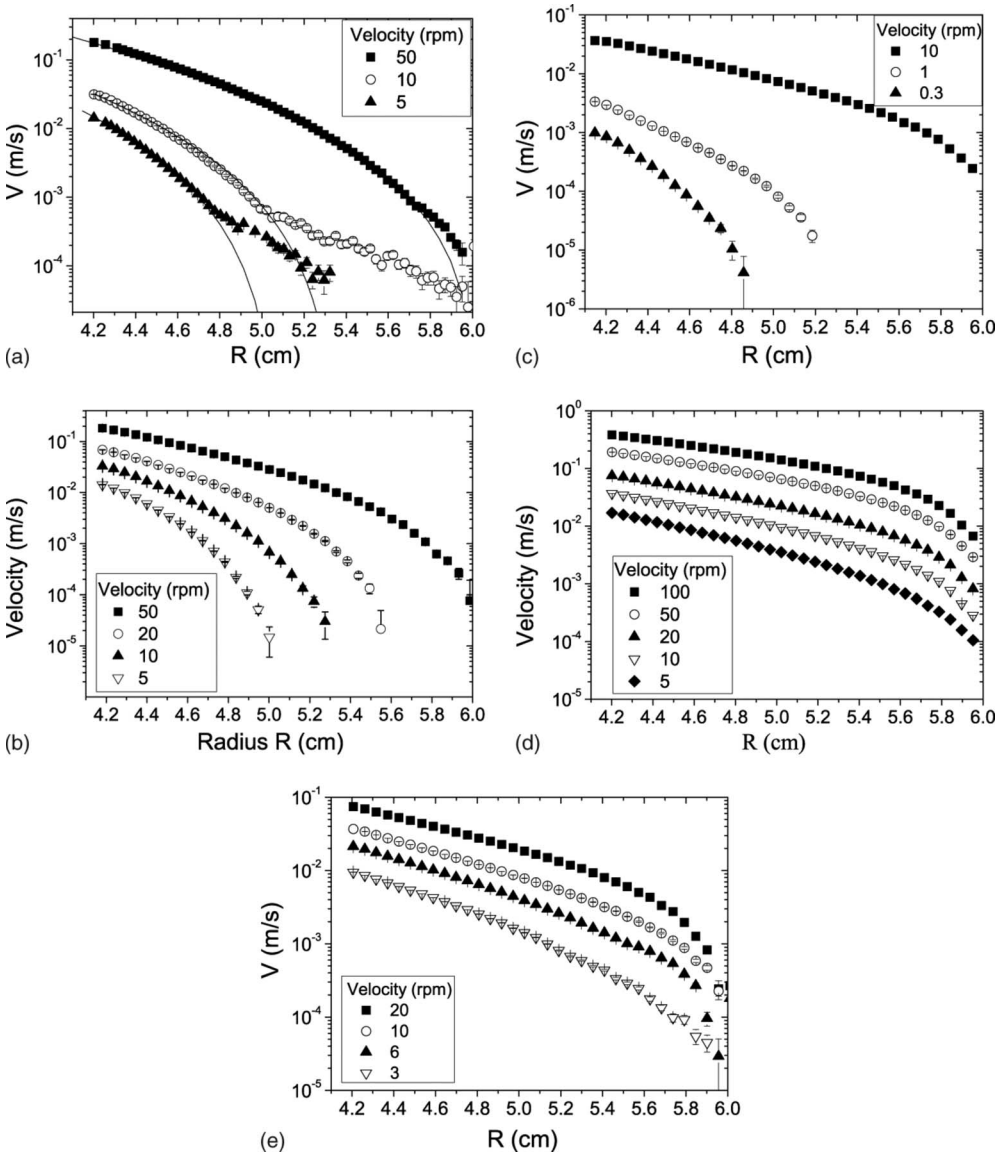


FIG. 3. The same plots as in Fig. 2 in log scale (for readability, not all profiles are plotted). The solid lines of Fig. 3(a) are the velocity profiles predicted by a Herschel-Bulkley law.

$$\Omega = \int_{R_i}^{R_o} \dot{\gamma}(R)/R dR, \tag{6}$$

where $R_i$ is the inner radius and $R_o$ is the outer radius. From Eqs. (5) and (6), we see that from the knowledge of the torque $T$ and the rotational velocity $\Omega$, we obtain a non-straightforward relationship between the local shear stress and the local shear rate. In order to go one step further, Eqs. (5) and (6) may be combined into

$$\Omega = -\frac{1}{2}\int_{\tau(R_i)}^{\tau(R_o)} \dot{\gamma}(\tau)/\tau d\tau. \tag{7}$$

Note that the possibility of shear localization is naturally taken into account in this equation, where $\dot{\gamma}(R)=0$ when $\tau(R)<\tau_c$ with $\tau_c$ the material yield stress. The constitutive law may then be derived from the whole macroscopic rheometric curve $T(\Omega)$ thanks to the differentiation of Eq. (7) relative to $T$:

$$2T\partial\Omega/\partial T = \dot{\gamma}[\tau(R_i)] - \dot{\gamma}[\tau(R_o)]. \tag{8}$$

Finally, in order to get the shear rate $\dot{\gamma}[\tau(R_i)]$ at the inner cylinder as a function of the shear stress at the inner cylinder, one needs to eliminate the shear rate at the outer cylinder $\dot{\gamma}[\tau(R_o)]$ from this equation. This can be done by summing this relationship with a series of successive decreasing torques (that differ by a factor $R_i^2/R_o^2$ at each step) chosen to ensure that the shear rate at the outer cylinder is eliminated in the summation at each step, until a zero shear rate is reached at the outer cylinder: the summation stops when the shear stress computed at the outer cylinder at a given step falls below the yield stress [6]. While this summation is in principle infinite for simple fluids, only a few steps are needed in the case of yield stress fluids, and the number of

steps is more reduced for wider gaps. In the case of our Couette geometry, as the ratio between the shear stress at the inner cylinder and the shear stress at the outer cylinder $(R_i^2/R_o^2)$ is equal to 2.1, we see that the data of Fig. 4(a) can be easily processed thanks to a maximum number of two summations of Eq. (8). From Eq. (7), note that such analysis is based on the assumption that there is a local constitutive law characterizing the material and that there is negligible wall slip.

The constitutive law obtained with this method is depicted in Fig. 4(b). We observe that the behavior of the material obtained with this procedure is basically well fitted to a Herschel-Bulkley law. In Sec. III D we compare this law to the constitutive law built from the local shear rates extracted from the velocity profiles.

### D. Local constitutive laws

#### *1. Local measurements*

The constitutive laws of the materials accounting for their velocity profiles can be built from our experimental data, using both the velocity profiles and the torque measurements. The stress distribution $\tau(R)$ within the gap is obtained from the macroscopic torque measurements thanks to Eq. (5). The local shear rate $\dot{\gamma}(R)$ in the gap is inferred from the velocity profiles $V(R)$ through

$$\dot{\gamma}(R) = V/R - \partial V/\partial R. \tag{9}$$

Both measurements performed at a given radius $R$ for a given rotational velocity $\Omega$ thus provide a local data point of the constitutive law $\tau = f(\dot{\gamma})$. This analysis provides a fair local measurement of the constitutive law since we measure the true local shear rate within the bulk of the material and the shear stress distribution is known from the momentum balance independently of any hypothesis; in particular, it is independent of what happens at the interface so that a possible wall slip does not affect this analysis. We are finally allowed to combine the data measured at various radiuses because the materials are homogeneous, as shown in Sec. III A.

The local constitutive law extracted from the experiments performed at various rotational velocities $\Omega$ on all the emulsions are plotted in Fig. 5 (we could not analyze the data for the 40-$\mu$m emulsion as torque data could not be measured in this case).

It should first be noted that for each emulsion, all the shear stress vs shear rate data fall along a single curve. This means that for a given material, our different data obtained under different boundary conditions effectively reflect the behavior of a single material with a given intrinsic constitutive law in simple shear. Note also that this is consistent with the absence of migration: any heterogeneity would have apparently yielded different constitutive laws for different rotational velocities [10,12]. Our observation of a single local constitutive law accounting for all flows of the nonadhesive 6.5-$\mu$m emulsion [Fig. 5(a)] contrasts with the observations of Goyon *et al.* [4] on the same system in microchannel flows of up to 250-$\mu$m width: the velocity profiles observed in the channel cannot be accounted for by a single constitutive law. This apparent paradox has been solved by Goyon *et al.* [4]: they showed that a rather simple nonlocal flow rule accounts for all the velocity profiles. They concluded that nonlocal effects should be observable in a zone involving up to 100 particles; beyond this zone, this nonlocal law reduces to a local law. This explains why our measurements are unsensitive to such effects and why we measure a single local constitutive law: using a wide-gap geometry prevents us from being sensitive to these nonlocal effects. Our observation of a single local constitutive law accounting for all flows of the adhesive 0.3-$\mu$m emulsion [Fig. 5(b)] also contrasts with the observations of Bécu *et al.* [3]. On exactly the same 0.3-$\mu$m adhesive emulsion sheared in a thin-gap Couette geometry, Bécu *et al.* [3] were actually unable to fit all their velocity profiles with a single constitutive law. In the Bécu *et al.* [3] study, the gap being 1 mm for 0.3 $\mu$m droplets, the nonlocal effects evidenced by Goyen *et al.* [4] cannot be the reason for the apparent absence of a single constitutive law accounting for all flows. An important point should be noted that may explain the differences between both studies of the same material: the experimental procedures are slightly different, and the time evolutions of the emulsion properties are very different. In our experiments, the emulsion was first presheared with a mixer and then at 100 rpm for 5 minute in

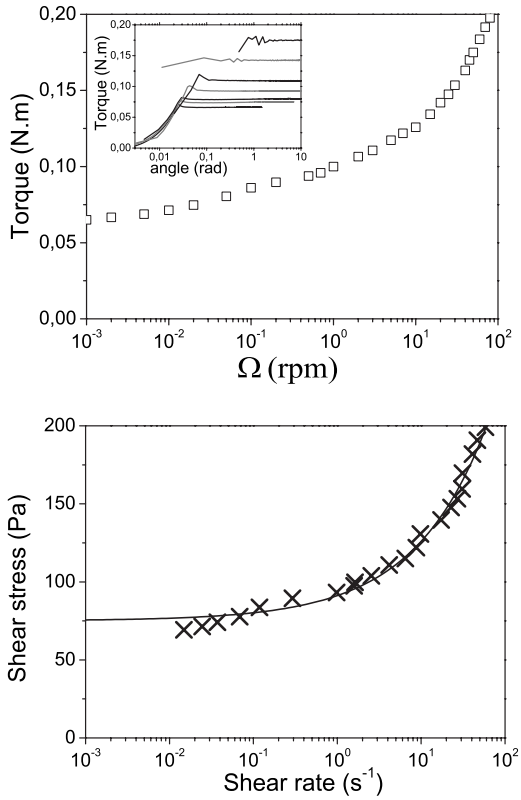


FIG. 4. (a) Macroscopic measurements: stationary torque vs rotational velocity for the steady flows of a 0.3-$\mu$m adhesive emulsion; inset: torque vs angular displacement for various rotational velocities ranging between 0.01 and 50 rpm (bottom to top). (b) Constitutive law inferred from the purely macroscopic measurements thanks to Eqs. (5) and (8); the solid line is a Herschel-Bulkley fit $\tau = \tau_c + \eta_{HB}\dot{\gamma}^n$ of the data with $\tau_c = 77$ Pa, $\eta_{HB} = 15.4$ Pa s, and $n = 0.5$.

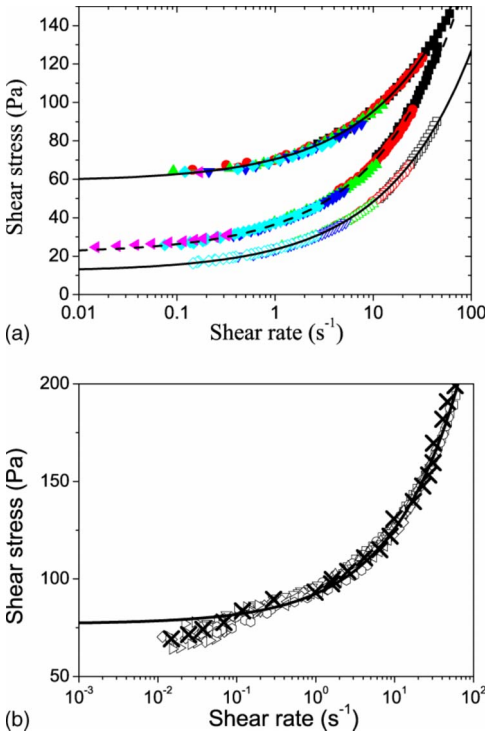


FIG. 5. (Color online) (a) Constitutive law measured locally in the gap of a Couette cell for the flows of (from top to bottom) a nonadhesive 1-$\mu$m emulsion, a nonadhesive 6.5-$\mu$m emulsion, and an adhesive 6.5-$\mu$m emulsion; the solid line is a Herschel-Bulkley fit $\tau=\tau_c+\eta_{HB}\dot{\gamma}^n$ of the data with $n=0.5$ for all materials, $\tau_c=59$ Pa and $\eta_{HB}=11.5$ Pa s for the nonadhesive 1-$\mu$m emulsion, $\tau_c=12$ Pa and $\eta_{HB}=11.5$ Pa s for the nonadhesive 6.5-$\mu$m emulsion, and $\tau_c=21.5$ Pa and $\eta_{HB}=15$ Pa s for the adhesive 6.5-$\mu$m emulsion. (b) Constitutive law measured locally in the gap of a Couette cell for the flows of a 0.3-$\mu$m adhesive emulsion (empty symbols); the solid line is a Herschel-Bulkley fit $\tau=\tau_c+\eta_{HB}\dot{\gamma}^n$ of the data with $\tau_c=77$ Pa, $\eta_{HB}=15.4$ Pa s, and $n=0.5$. The crosses are the data extracted from the analysis of the purely macroscopic measurements [see Fig. 4(b)].

a Couette cell with rough surfaces. The stationary velocity profiles then measured at various rotational velocities were found to develop within a few seconds and to remain stable for hours. In the experimental procedure of Bécu *et al.* [3], each experiment is conducted on a fresh sample which is directly sheared at the studied shear rate during at least 3 h. A key point may then be that Bécu *et al.* [3] found their system to evolve for at least two hours, in contrast with our observations: whatever the rotational velocity, they found the apparent viscosity of the system to decrease slowly in time. This would mean that their material was in an initially structured state, and was destructured by shear, whatever the magnitude of the shear rate. Then, while the authors claim that the velocity profiles no longer change significantly after 2 h, one may think that some slow relaxation still occurs and that the steady state is not really reached. This would mean that the measurements performed at different rotational velocities have been performed on different structural states of the emulsion (in contrast with our measurements), naturally leading to different constitutive laws for the different velocities studied. This explanation based on the influence of the initial state of the material would be consistent with the observations of Ragouilliaux *et al.* [11] who showed that simple emulsions whose flow properties show no apparent thixotropic effects when first presheared at high shear rate are actually subject to significant aging at rest: this implies in particular that such systems have to be strongly presheared before any study. This preshear was performed in our study; it was not in the Bécu *et al.* [3] study. Two other points may be noted: first, although the composition of the two emulsions is the same, the samples are different and chemical impurities may play an important role in the adhesion process; second, the Couette cell used by Bécu *et al.* [3] is smooth and huge wall slip is evidenced.

Focusing on the nonadhesive 1 $\mu$m, the adhesive 6.5 $\mu$m, and the nonadhesive 6.5 $\mu$m emulsions, we observe that the behavior of all materials is well fitted to a Herschel-Bulkley behavior $\tau=\tau_c+\eta_{HB}\dot{\gamma}^n$ of index $n=0.5$ in all the range of measured shear rates; this is consistent with previous observations of the behavior of dense emulsions [2,44]. Coming back to the 0.3-$\mu$m adhesive emulsion, at moderate and high shear rates (above 0.1 s$^{-1}$), the behavior is the same as the one encountered for the large droplets emulsions: the constitutive law is well fitted to a Herschel-Bulkley law on index $n=0.5$.

At low shear rate (in a 0.01–0.1-s$^{-1}$ range), the behavior of the 0.3-$\mu$m adhesive emulsion differs from the previous ones. All the points still fall on the same curve but a slight slope break is noticed in the flow curve. While a stress plateau should be reached for a simple yield stress fluid, the shear stress continues decreasing when the shear rate decreases. This is also observed on the law inferred from the macroscopic measurement. As far as we can say, this behavior is specific to the 0.3-$\mu$m adhesive emulsion: we took care of measuring the local behavior at low shear rates in the 6.5-$\mu$m adhesive emulsion but observed no slope break for shear rates as low as $10^{-2}$ s$^{-1}$. A probable reason for the differences observed between these systems is that the 0.3-$\mu$m emulsion is more adhesive than the others, in particular because of their larger surface to volume ratio. This low shear rate behavior corresponds to the slow flows observed below a first apparent yield stress in Fig. 3(a). At low rotational velocity, when there is apparently shear localization, the velocity profiles are well fitted to the Herschel-Bulkley law predictions only for velocities larger than a few 100 $\mu$m s$^{-1}$. For lower velocities, at the approach of the radius where the yield stress should be reached and the velocity should tend to zero, the velocity starts to decrease very slowly with the radius; on the other hand, at high rotational velocity, when all the gap is sheared, the velocity profile is very well fitted to the Herschel-Bulkley law prediction. The analysis of this behavior is difficult. One may think that the emulsion flows homogeneously and really follows a single continuous local constitutive law that corresponds to a Herschel-Bulkley equation at high shear rate and differs from this equation at low shear rate. One may also suggest that the law at low shear rates does not correspond to steady flows. Indeed, it has to be noted that the measurements of the very low velocities in Fig. 3(a) are averages over 1 min: we cannot know if they correspond to steady flows (the measure-

ments may, e.g., reflect a stick-slip behavior). These flows may thus reflect the existence of a jammed phase perturbated by some unsteady local rearrangements. In this case, this behavior would be reminiscent of shear banding, which has already been observed for strongly adhesive emulsions [11] and is explained by a competition between structuration due to the adhesion process and destructuration by shear [6,11].

#### *2. Comparison between local measurements and purely macroscopic measurements*

The local measurements obtained for the 0.3-$\mu$m adhesive emulsion are compared in Fig. 5(a) with the law inferred from the purely macroscopic measurements (see Sec. III C). We observe that both laws are very well matched. In particular, the macroscopic measurements also allow us to evidence the slope break in the constitutive law at low shear rate. This validate the use of a wide-gap Couette geometry as a tool to obtain the constitutive law of dense emulsions from purely macroscopic rheometrical measurements, provided that a proper analysis of the macroscopic data is performed. We recall that this agreement is due to four important features: (i) we have shown that all dense emulsions seem to be free from migration and thus remain homogeneous during the experiments, (ii) the use of a wide gap prevents from the nonlocal effects observed by Goyon *et al.* [4], (iii) the material is initially destructured and a steady state is studied (this may have not been the case in the Bécu *et al.* [3] study), (iv) wall slip has to be negligible to allow for a proper analysis of the macroscopic data: this is ensured here by the use of rough walls of roughness larger than the droplet size, as shown below.

#### *3. Wall slip*

As pointed out in Sec. III B, our velocity measurement method does not provide the velocity at the walls: the first reliable data are obtained at around 0.5–1 mm from the inner cylinder. However, the local measurements of the constitutive law we have performed make it possible to study in more detail a possible wall slip effect. For a given rotational velocity of the inner cylinder, the velocity of the emulsion expected at the walls can actually be computed thanks to the knowledge of the shear rate in the emulsion corresponding to the shear stress value at the wall. The same shear stress level was actually reached somewhere in the bulk of the material for a higher rotational velocity of the inner cylinder, and the shear rate corresponding to this shear stress was then measured locally thanks to the velocity profile measurement. The velocity profile expected in the zone near the inner cylinder can then be reconstructed from the velocity profile measured at some distance from the walls and from the expected shear rate near the wall. Of course, this analysis is based on the hypothesis that the material is the same as in the bulk in this 0.5–1-mm zone near the walls, which may be no more true in a zone where there are nonlocal effects [4]. Note also that this method can be used only when the reproducibility of the experiments is very good (allowing data measured at a given rotational velocity to be used to predict what happens at another velocity). An example of this method applied to the flows of the 6.5-$\mu$m adhesive emulsion is depicted in Fig. 6.

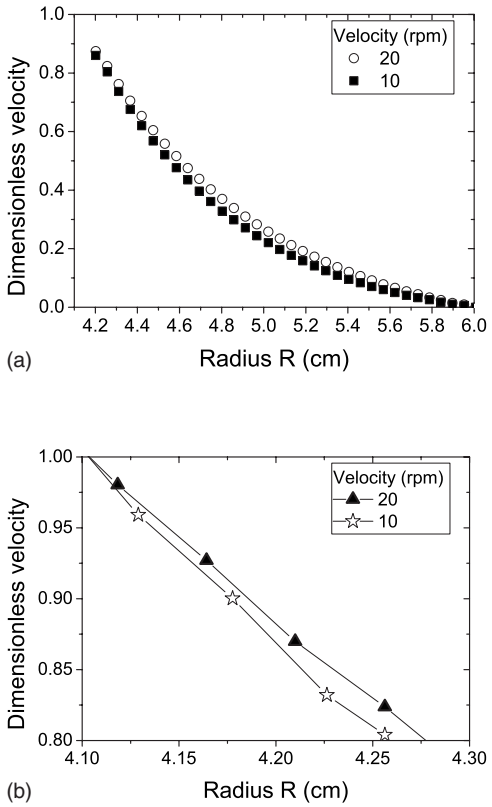


FIG. 6. (a) Dimensionless velocity profiles for the steady flows of a 6.5-$\mu$m adhesive emulsion, for a 10- and a 20-rpm rotational velocity. (b) Dimensionless velocity profiles expected near the walls at 10 and 20 rpm; the velocities are computed thanks to the local shear rate measurements performed at 50 rpm.

We observe in Fig. 6(b) that the dimensionless velocity profiles expected near the walls have a value that is very close to 1. This analysis was performed on several velocity profiles, and in all cases the dimensionless velocity values predicted at the inner cylinder were found to be equal to 1 within 1%. We finally conclude that, thanks to the use of rough surfaces of roughness larger than the droplet size, there is probably no wall slip in our experiments; if any, it is of order 1% or less. This feature shows that the macroscopic measurements performed with a wide-gap Couette rheometer with rough walls can be trusted: this explains the very good agreement observed in Fig. 5(a) between the constitutive law measured locally and the constitutive law inferred from the purely macroscopic measurements.

## IV. CONCLUSION

We have studied the flows of several dense emulsions in a wide-gap Couette geometry. We have coupled macroscopic rheometric experiments and local velocity and concentration measurements through MRI techniques. The method devoted to measure the local droplet concentration was developed specifically for this study. In contrast with dense suspensions of rigid particles where very fast migration occurs under shear, we showed that no migration takes place in dense

emulsions even for strain as large as 100 000 in our systems. This may imply that another mechanism is involved in dense emulsions than in dense suspensions. The homogeneity of our materials under shear allows to infer their constitutive law from purely macroscopic measurements. This constitutive law is consistent with the one inferred from the velocity profiles. This contrasts with previous results obtained by Goyon *et al.* [4] within a microchannel where nonlocal finite size effects are likely to have prevented us from obtaining a constitutive law. It also differs from the results of Bécu *et al.* [3], where the loading procedure probably prevented the authors to reach a steady state. We thus suggest that properly analyzed purely macroscopic measurements in a wide-gap Couette geometry can be used as a tool to study dense emulsions. All behaviors we observed are basically consistent with Herschel-Bulkley laws of index 0.5. However, we also evidence the existence of discrepancies with this law at the approach of the yield stress due to slow shear flows in the case of strongly adhesive emulsions, whose physical origin is unclear. Finally, we have shown that there is probably no wall slip.

## ACKNOWLEDGMENTS

We thank Sébastien Manneville for fruitful discussions. Financial support of Rhodia and Région Aquitaine is acknowledged.

[1] R. G. Larson, *The Structure and Rheology of Complex Fluids* (Oxford University Press, New York, 1999).
[2] T. G. Mason, J. Bibette, and D. A. Weitz, J. Colloid Interface Sci. **179**, 439 (1996).
[3] L. Bécu, S. Manneville, and A. Colin, Phys. Rev. Lett. **96**, 138302 (2006).
[4] J. Goyon, A. Colin, G. Ovarlez, A. Ajdari, and L. Bocquet, Nature (London) **454**, 84 (2008).
[5] J. B. Salmon, L. Bécu, S. Manneville, and A. Colin, Eur. Phys. J. E **10**, 209 (2003).
[6] P. Coussot, *Rheometry of Pastes, Suspensions and Granular Materials* (John Wiley & Sons, New York, 2005).
[7] P. C. F. Møller, J. Mewis, and D. Bonn, Soft Mater. **2**, 274 (2006).
[8] P. Coussot, J. S. Raynaud, F. Bertrand, P. Moucheront, J. P. Guilbaud, H. T. Huynh, S. Jarny, and D. Lesueur, Phys. Rev. Lett. **88**, 218301 (2002).
[9] J. S. Raynaud, P. Moucheront, J. C. Baudez, F. Bertrand, J. P. Guilbaud, and P. Coussot, J. Rheol. **46**, 709 (2002).
[10] N. Huang, G. Ovarlez, F. Bertrand, S. Rodts, P. Coussot, and D. Bonn, Phys. Rev. Lett. **94**, 028301 (2005).
[11] A. Ragouilliaux, G. Ovarlez, N. Shahidzadeh-Bonn, B. Herzhaft, T. Palermo, and P. Coussot, Phys. Rev. E **76**, 051408 (2007).
[12] G. Ovarlez, F. Bertrand, and S. Rodts, J. Rheol. **50**, 259 (2006).
[13] K. G. Hollingsworth and M. L. Johns, J. Rheol. **48**, 787 (2004).
[14] A. Ragouilliaux, B. Herzhaft, F. Bertrand, and P. Coussot, Rheol. Acta **46**, 261 (2006).
[15] G. Picard, A. Ajdari, F. Lequeux, and L. Bocquet, Phys. Rev. E **71**, 010501(R) (2005).
[16] A. Karnis and S. G. Mason, J. Colloid Interface Sci. **24**, 164 (1967).
[17] K. G. Hollingsworth and M. L. Johns, J. Colloid Interface Sci. **296**, 700 (2006).
[18] S. D. Hudson, Phys. Fluids **15**, 1106 (2003).
[19] M. R. King and D. T. Leighton, Jr., Phys. Fluids **13**, 397 (2000).
[20] A. M. Corbett, R. J. Phillips, R. J. Kauten, and K. L. McCarthy, J. Rheol. **39**, 907 (1995).
[21] A. L. Graham, S. A. Altobelli, E. Fukushima, L. A. Mondy, and T. S. Stephens, J. Rheol. **35**, 191 (1991).
[22] D. Leighton and A. Acrivos, J. Fluid Mech. **181**, 415 (1987).
[23] R. J. Phillips, R. C. Armstrong, R. A. Brown, A. L. Graham, and J. R. Abbott, Phys. Fluids A **4**, 30 (1992).
[24] C. Barentin, E. Azanza, and B. Pouligny, Europhys. Lett. **66**, 139 (2004).
[25] M. K. Lyon and L. G. Leal, J. Fluid Mech. **363**, 25 (1998).
[26] S. W. Sinton and A. W. Chow, J. Rheol. **35**, 735 (1991).
[27] P. Mills and P. Snabre, J. Phys. II **5**, 1597 (1995).
[28] P. Nott and J. F. Brady, J. Fluid Mech. **275**, 157 (1994).
[29] T. G. Mason and J. Bibette, Phys. Rev. Lett. **77**, 3481 (1996).
[30] S. Rodts, F. Bertrand, S. Jarny, P. Poullain, and P. Moucheront, C. R. Chim. **7**, 275 (2004).
[31] J. Götz and K. Zick, Chem. Eng. Technol. **26**, 59 (2003).
[32] S. L. Duce, S. Ablett, T. M. Guiheneuf, M. A. Horsfield, and L. D. Hall, J. Food. Sci. **59**, 808 (1994).
[33] S. Yao, M. Costello, A. G. Fane, and J. M. Pope, J. Membr. Sci. **99**, 207 (1995).
[34] M. A. D'Avila, N. C. Shapley, J. H. Walton, R. J. Philipps, S. R. Dungan, and R. L. Powell, Phys. Fluids **15**, 2499 (2003).
[35] M. L. Johns and K. G. Hollingsworth, Prog. Nucl. Magn. Reson. Spectrosc. **50**, 51 (2007).
[36] R. J. Kauten, J. E. Maneval, and M. J. McCarthy, J. Food. Sci. **56**, 799 (1991).
[37] L. Marciani, M. Wickham, B. P. Hills, J. Wright, D. Bush, R. Faulks, A. Fillery-Travis, R. C. Spiller, and P. A. Gowland, J. Food. Sci. **69**, E290 (2004).
[38] B. Newling, P. M. Glover, J. L. Keddie, D. M. Lane, and P. J. McDonald, Langmuir **13**, 3621 (1997).
[39] A. Acrivos, J. Rheol. **39**, 813 (1995).
[40] D. Leighton and A. Acrivos, J. Fluid Mech. **177**, 109 (1987).
[41] J. R. Abbott, N. Tetlow, A. L. Graham, S. A. Altobelli, E. Fukushima, L. A. Mondy, and T. S. Stephens, J. Rheol. **35**, 773 (1991).
[42] N. Tetlow, A. L. Graham, M. S. Ingber, S. R. Subia, L. A. Mondy, and S. A. Altobelli, J. Rheol. **42**, 307 (1998).
[43] J. F. Morris and F. Boulay, J. Rheol. **43**, 1213 (1999).
[44] S. P. Meeker, R. T. Bonnecaze, and M. Cloitre, J. Rheol. **48**, 1295 (2006).